

Gold Nanoshells on Polystyrene Cores for Control of Surface Plasmon Resonance

Weili Shi,^{†,§} Y. Sahoo,^{‡,§} Mark T. Swihart,^{†,§} and P. N. Prasad^{*,‡,§}

Department of Chemical and Biological Engineering and Department of Chemistry and The Institute for Lasers, Photonics, and Biophotonics, University at Buffalo (SUNY), Buffalo, New York 14260

Received September 23, 2004. In Final Form: November 5, 2004

A method is presented for synthesizing core–shell structures consisting of monodisperse polystyrene latex nanospheres as cores and gold nanoparticles as shells. Use of polystyrene spheres as the core in these structures is advantageous because they are readily available commercially in a wide range of sizes, and with dyes or other molecules doped into them. Gold nanoparticles, ranging in size from 1 to 20 nm, are prepared by reduction of a gold precursor with sodium citrate or tetrakis(hydroxymethyl)phosphonium chloride (THPC). Carboxylate-terminated polystyrene spheres are functionalized with 2-aminoethanethiol hydrochloride (AET), which forms a peptide bond with carboxylic acid groups on their surface, resulting in a thiol-terminated surface. Gold nanoparticles then bind to the thiol groups to provide up to about 50% coverage of the surface. These nanoparticles serve as seeds for growth of a continuous gold shell by reduction of additional gold precursor. The shell thickness and roughness can be controlled by the size of the nanoparticle seeds as well as by the process of their growth into a continuous shell. By variation of the relative sizes of the latex core and the thickness of the gold overlayer, the plasmon resonance of the nanoshell can be tuned to specific wavelengths across the visible and infrared range of the electromagnetic spectrum, for applications ranging from the construction of photonic crystals to biophotonics. The position and width of the plasmon resonance extinction peak are well-predicted by extended Mie scattering theory.

Introduction

Recent intense interest in nanoparticles and other nanostructures stems from the fact that, unlike bulk materials, their properties—optical, electronic, mechanical, and chemical—may depend on their size and geometry. This provides an additional degree of freedom in preparing materials with desired properties and can allow combinations of properties not attainable with conventional materials. Nanoparticles of metallic, semiconducting, and magnetic materials have generated research interest lately because of their potential uses in optoelectronics, reprography, catalysis, chemical, and biological sensing, etc. Among the metallic particles, the study of colloidal gold particles stands out in particular. It is one of the most widely studied systems for which interest can be traced back to the time of Faraday. At present, there exist well-established methods to prepare stable colloidal solutions of gold nanoparticles in both polar and nonpolar solvents.^{1–4}

Gold nanoparticles are used in a variety of applications based on their optical and electronic properties, particularly their strong surface plasmon resonance (SPR) absorption in aqueous media around 520 nm. The strong SPR is due to the high electronic polarizability of small particles, which yields a very high extinction coefficient. The resonance frequency is dependent on the size, shape,

material properties, surrounding medium, and the state of aggregation of the nanoparticles.⁵ The SPR absorption and other unique properties resulting from their small size can be exploited in a range of applications in bioimaging, chemical and biological sensing, optical filters⁶ and single-electron transistors.⁷ The ability to shift the SPR, in a controlled fashion, to the spectral region best suited for optical bioimaging and biosensing applications would open the way to numerous additional bioapplications.⁸

A geometry that has drawn great interest recently is the metallic nanoshell, which consists of a dielectric spherical core, surrounded by a thin, uniform metallic shell.⁹ This nanostructure has the unique optical property that by changing the relative sizes of the core and the shell, its SPR can be broadly tuned.⁹ Halas and co-workers have developed a procedure to make gold nanoshells on silica treated with (aminopropyl)triethoxysilane.^{9,10} Furthermore, they designed the gold nanoshells to absorb infrared light and used them for biomedical applications such as thermal ablative cancer therapy, immunoassays within complex biomedica, and photothermally assisted drug delivery, etc.^{11–14} They have recently extended this

* Corresponding author. Telephone: (716) 645-6800 x2098. Fax: (716) 645-6945. E-mail: pnprasad@buffalo.edu.

[†] Department of Chemical and Biological Engineering.

[‡] Department of Chemistry.

[§] The Institute for Lasers, Photonics, and Biophotonics.

(1) Grabar, K. C.; Smith, P. C.; Musick, M. D.; Davis, J. A.; Walter, D. G.; Jackson, M. A.; Guthrie, A. P.; Natan, M. J. *J. Am. Chem. Soc.* **1996**, *118*, 1148.

(2) Templeton, A. C.; Chen, S. W.; Gross, S. M.; Murray, R. W. *Langmuir* **1999**, *15*, 66.

(3) Leff, D. V.; Brandt, L.; Heath, J. R. *Langmuir* **1996**, *12*, 4723.

(4) Brust, M.; Fink, J.; Bethell, D.; Schiffrin, D. J.; Kiely, C. *J. Chem. Soc., Chem. Commun.* **1995**, 1655.

(5) Prasad, P. N. *Nanophotonics*; Wiley: Hoboken, NJ, 2004; Chapter 5.

(6) Dirix, Y.; Bastiaansen, C.; Caseri, W.; Smith, P. *Adv. Mater.* **1999**, *11*, 223.

(7) Sato, T.; Hasko, D. G.; Ahmed, H. *J. Vac. Sci. Technol., B* **1997**, *15*, 45.

(8) Lim, Y. T.; Park, O. O.; Jung, H. T. *J. Colloid. Interface Sci.* **2003**, *263*, 449.

(9) Oldenburg, S. J.; Averitt, R. D.; Westcott, S. L.; Halas, N. J. *Chem. Phys. Lett.* **1998**, *288*, 243.

(10) Pham, T.; Jackson, J. B.; Halas, N. J.; Lee, T. R. *Langmuir* **2002**, *18*, 4915.

(11) Hirsch, L. R.; Jackson, J. B.; Lee, A.; Halas, N. J.; West, J. *Anal. Chem.* **2003**, *75*, 2377.

(12) Hirsch, L. R.; Stafford, R. J.; Bankson, J. A.; Sershen, S. R.; Rivera, B.; Price, R. E.; Hazle, J. D.; Halas, N. J.; West, J. L. *P. Natl. Acad. Sci. U.S.A.* **2003**, *100*, 13549.

(13) West, J. L.; Halas, N. J. *Curr. Opin. Biotech.* **2000**, *11*, 215.

(14) West, J. L.; Halas, N. J. *Annu. Rev. Biomed. Eng.* **2003**, *5*, 285.

method to produce multiple, concentric shells.¹⁵ They also demonstrated the use of gold nanoshells to reduce the oxidation rate of semiconducting polymers.¹⁶ Graf et al.¹⁷ modified Halas' synthesis procedure to make gold shells on silica and further encapsulated the gold nanoshells in silica to decrease the van der Waals forces between the particles and reduce aggregation. Jung's group⁸ used another method to make gold nanoshells on silica. They modified the silica surface with tin to seed gold nucleation and then reduced gold chloride to form a complete gold shell in a single step.

As described above, there are relatively well-developed methods for growing gold nanoshells on silica cores. However, there are few reports on the fabrication of gold shells on cores of other materials. Polystyrene spheres have been particularly useful for the formation of photonic crystals. Their high degree of uniformity makes them relatively easy to self-assemble into a uniform colloidal crystal, and the relatively high refractive index contrast between the spheres and air-filled voids between them allows for enhanced confinement of light.¹⁸ The higher refractive index of polystyrene, compared to silica, also results in a somewhat narrower plasmon resonance absorption peak for gold shells on polystyrene compared to gold shells on silica. Dye-doped polystyrene spheres are also readily available, and using them could provide another means of controlling the optical properties of the overall nanostructure. It may also be possible to pyrolyze the polystyrene core by laser heating, leaving a hollow nanoshell that could be refilled with another material. Halas' group has demonstrated reshaping of nanoshells on silica by laser-heating, with some modification of the silica core at the highest temperatures.^{19,20} Caruso's group has fabricated various metallic nanoshells on both silica and polystyrene cores using a layer-by-layer technique,^{21–25} and this approach has also been adopted in various forms by others.^{26–28} The process entails the sequential deposition of oppositely charged polyelectrolytes onto colloidal particles, exploiting primarily electrostatic interactions for polymer multilayer buildup, but involving a laborious procedure of removing nonbound polyelectrolytes and nanocrystals at each step of the assembly. This layer-by-layer method is ultimately effective and powerful, but much more cumbersome than the seed and grow method of shell formation used by Halas' group for preparing gold shells on silica particles.

Here, we present an alternative, relatively facile, seed and grow method for growth of controlled polystyrene core–gold shell nanostructures starting from commercially available carboxylate-terminated polystyrene mi-

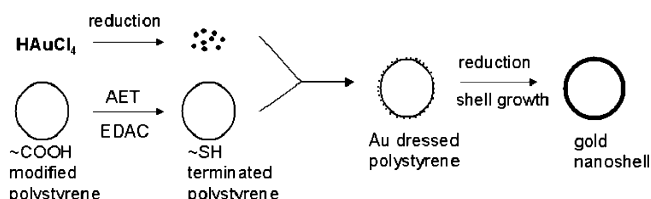


Figure 1. Schematic illustration of the synthesis of gold nanoshells.

crosheres and chemically modifying the surface for attachment to gold.

Experimental Section

(i) Materials. Carboxylate-modified polystyrene (296 nm, 10 wt % in water) was obtained from Seradyn OptiLink. 2-Aminoethanethiol hydrochloride ($\text{NH}_2\text{CH}_2\text{CH}_2\text{SH}\cdot\text{HCl}$, AET, 98%), tetrakis(hydroxymethyl)phosphonium chloride (THPC, 80% solution in water), hydroxylamine hydrochloride ($\text{NH}_2\text{OH}\cdot\text{HCl}$, 99%), and hydrogen tetrachloroaurate(III) trihydrate ($\text{HAuCl}_4\cdot 3\text{H}_2\text{O}$) were purchased from Aldrich. *N*-Ethyl-*N'*-(3-(dimethylamino)propyl)carbodiimide hydrochloride ($\text{C}_8\text{H}_{17}\text{N}_3\cdot\text{HCl}$, EDAC) and 2-(*N*-morpholino)ethanesulfonic acid (MES, >99.5%) were purchased from Sigma. Sodium citrate (dehydrate, granular) and potassium carbonate were purchased from J. T. Baker Inc. All chemicals were used as received. HPLC-grade water was used at every stage of reaction and washing.

(ii) Synthesis. An outline of the synthesis of gold nanoshells is shown schematically in Figure 1. Details are as follows:

(a) Functionalization of Polystyrene Nanoparticle Surface with AET. AET can be covalently attached to the surface of carboxylate-modified polystyrene particles. Carboxyl groups on the polystyrene particles, activated by the water-soluble carbodiimide EDAC, react with free amino groups of the adsorbed AET to form amide bonds. To accomplish this, 0.4 mL of MES stock buffer (500 mM, pH = 6.1) was added to 0.4 g of carboxylate-modified polystyrene (296 nm, 10 wt %) particle solution while vigorously stirring. A 3.2 mL aliquot of HPLC-grade water was added to the mixture to make the total volume 4 mL. Next, 3.5 mL of 52 $\mu\text{mol/mL}$ EDAC aqueous solution was added to the vigorously stirred mixture. The amount of EDAC required was calculated following the instructions of the polystyrene sphere manufacturer.²⁹ It is recommended that approximately a 0.5–2.5-fold molar excess over the microparticle carboxyl concentration be used. After 30 min, 15 mg of AET in 0.5 mL of HPLC water was added to the vigorously stirred mixture. The mixture was stirred for 3 h. EDAC and excess AET were removed from the AET-functionalized polystyrene particles by repeated centrifugation (10 000 rpm for 10 min), the precipitate being redispersed in 20 mL of HPLC water at least 3 times.

(b) Preparation of Colloidal Gold Nanoparticles. We prepared two types of colloidal gold nanoparticles, by reduction of chloroauric acid with sodium citrate and THPC, respectively, hereinafter called citrate–gold (about 12 nm in diameter) and THPC–gold (about 1–2 nm in diameter). Preparation of citrate–gold followed the method described by Hall et al.³⁰ To a flask containing 85 mL of boiling HPLC water, HAuCl_4 solution (10 mL, 5mM) was added, and the solution was allowed to return to a boil. A freshly prepared solution of sodium citrate (5 mL, 0.03 M) was then added to the flask. After a few minutes, the solution turned from colorless to a deep wine-red color. Heating was stopped at this point and the resulting sol left to cool overnight. The method described by Pham et al.¹⁰ was adopted for the preparation of THPC–gold. A 0.5 mL aliquot of 1 M NaOH and 1 mL of THPC solution (prepared by adding 12 μL of 80% THPC in water to 1 mL of HPLC-grade water) were added to 45 mL of HPLC water. The reaction mixture was stirred for 5 min, and 10 mL of 5mM HAuCl_4 was added rapidly to the stirred solution. The color changed to dark brown, indicating the formation of small (~ 2 nm) gold nanoparticles.

(15) Prodan, E.; Radloff, C.; Halas, N. J.; Nordlander, P. *Science* **2003**, *302*, 419.

(16) Hale, G. D.; Jackson, J. B.; Shmakova, O. E.; Lee, T. R.; Halas, N. J. *Appl. Phys. Lett.* **2001**, *78*, 1502.

(17) Graf, C.; van Blaaderen, A. *Langmuir* **2002**, *18*, 524.

(18) Gates, B.; Xia, Y. N. *Adv. Mater.* **2000**, *12*, 1329.

(19) Aguirre, C. M.; Moran, C. E.; Young, J. F.; Halas, N. J. *J. Phys. Chem. B* **2004**, *108*, 7040.

(20) Charnay, C.; Lee, A.; Man, S. Q.; Moran, C. E.; Radloff, C.; Bradley, R. K.; Halas, N. J. *J. Phys. Chem. B* **2003**, *107*, 7327.

(21) Salgueirino-Maceira, V.; Caruso, F.; Liz-Marzan, L. M. *J. Phys. Chem. B* **2003**, *107*, 10990.

(22) Liang, Z. J.; Susha, A.; Caruso, F. *Chem. Mater.* **2003**, *15*, 3176.

(23) Caruso, F. *Adv. Mater.* **2001**, *13*, 11.

(24) Caruso, F.; Spasova, M.; Saigueirino-Maceira, V.; Liz-Marzan, L. M. *Adv. Mater.* **2001**, *13*, 1090.

(25) Cassagneau, T.; Caruso, F. *Adv. Mater.* **2002**, *14*, 732.

(26) Dong, A. G.; Wang, Y. J.; Tang, Y.; Ren, N.; Yang, W. L.; Gao, Z. *Chem. Commun.* **2002**, 350.

(27) Dokoutchaev, A.; James, J. T.; Koene, S. C.; Pathak, S.; Prakash, G. K. S.; Thompson, M. E. *Chem. Mater.* **1999**, *11*, 2389.

(28) Ji, T. H.; Lirtsman, V. G.; Avny, Y.; Davidov, D. *Adv. Mater.* **2001**, *13*, 1253.

(29) *Recommended Adsorption and Covalent Coupling Procedures*; Seradyn, Inc.: Indianapolis, IN, 1999.

(30) Hall, S. R.; Davis, S. A.; Mann, S. *Langmuir* **2000**, *16*, 1454.

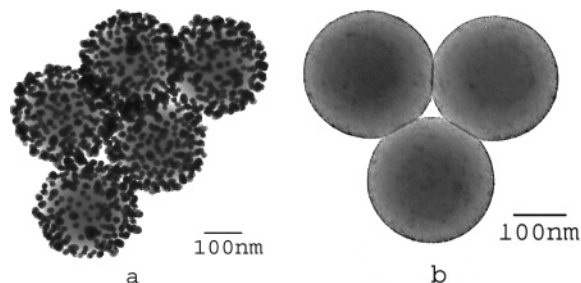


Figure 2. TEM images of 296 nm polystyrene spheres with (a) \sim 12 nm citrate-gold and (b) 1–2 nm THPC-gold attached to their surface.

(c) *Attachment of Gold Nanoparticles to AET-Functionalized Polystyrene Particles.* To attach citrate-gold to AET-modified polystyrene, 20 mL of the AET-polystyrene solution and 200 mL of citrate-gold aqueous solution were mixed with vigorous stirring, leading to the attachment of citrate-gold nanoparticles on the thiol groups of the AET-modified polystyrene. To remove the remaining free gold nanoparticles, the above solution was centrifuged, the supernatant was removed, and the remaining light brown pellet was redispersed in HPLC water. This centrifugation/re-dispersion step was repeated several times. This solution was further filtered three times using an Isopore polycarbonate membrane filter with 200 nm nominal pore size. Finally, the precipitate was re-dispersed in 100 mL of water. This meticulous removal of free gold particles is necessary because these particles will grow during the subsequent shell formation and thereby reduce the effectiveness and reproducibility of the shell formation process. The final result of this procedure was citrate-dressed polystyrene spheres such as those shown in Figure 2a. The citrate-gold dressed polystyrene particles remained dispersed in water for only a few hours. After that, aggregates formed that could only be broken up by ultrasonication. It was noted that the above ratio of AET-polystyrene to citrate-gold gives the maximum gold coverage on polystyrene. When the ratio decreased, we found polystyrene particles incompletely covered by gold nanoparticles. Their absorption shifted to shorter wavelength, as shown in Figure 9a.

To attach THPC-gold nanoparticles to the AET-modified polystyrene, 20 mL of the AET-polystyrene solution and 50 mL of the THPC-gold aqueous solution were mixed together with vigorous stirring. Excess gold nanoparticles were removed in the same manner as that described above for the citrate-gold dressed particles. Finally, the THPC-gold dressed particles were dispersed in 100 mL of water. The result of this procedure was THPC-gold dressed particles such as those shown in Figure 2b. We find that the dispersibility of THPC-gold dressed polystyrene in water is much better than that of citrate-gold dressed polystyrene, and the THPC-gold dressed particles were found to stay dispersed in water for at least several weeks.

(d) *Shell Growth.* Both citrate-gold and THPC-gold dressed polystyrene (Au/AET/PS) particles were used as seeds to form continuous gold shells. For this reaction step a method modified from Graf et al.¹⁷ and Pham et al.¹⁰ was executed. To grow the gold overlayer on the seed (Au/AET/PS) nanoparticles, we first prepared a solution of gold hydroxide.^{31–33} In a reaction flask, we dissolved 0.05 g of potassium carbonate (K_2CO_3) in 185 mL of HPLC-grade water. After 10 min of stirring, 15 mL of 5 mM $HAuCl_4$ was added to the solution. The mixture initially appeared transparent yellow and slowly became colorless after 30 min, indicating the formation of gold hydroxide.^{31–33} The resulting solution was aged for 24 h in the dark before being used in subsequent steps. In a typical preparation, 20 mL of the gold hydroxide solution was added to a 1 mL aliquot of Au/AET/PS particle solution. The amount of gold hydroxide solution was varied according to the intended thickness of the gold shell. To this vigorously stirred mixture, 10 mL of freshly prepared 1.87

mM hydroxylamine hydrochloride solution was added dropwise. This resulted in a black precipitate. After removing the upper purple solution, the precipitate was purified further by repeated cycles of centrifuging at low speed (1000 rpm) and removing the supernatant, before finally re-dispersing the precipitate in water.

(iii) **Characterization.** (a) *UV-Vis Absorbance.* Absorbance spectra were measured using a Shimadzu model 3101PC UV-vis-near-IR scanning spectrophotometer. Aliquots of various samples were measured against water as reference.

(b) *Transmission Electron Microscopy.* Transmission electron microscopy (TEM) images were obtained with a JEOL model JEM-100CX microscope at an acceleration voltage of 80 kV. The specimens were prepared by dropping the aqueous dispersion onto an amorphous carbon-coated 300-mesh copper grid and allowing the solvent to evaporate.

(c) *Scanning Electron Microscopy.* Scanning electron microscopy (SEM) images were obtained by using a Hitachi S4000 field emission microscope at an acceleration voltage of 20 kV. The nanoparticle dispersion was drop-cast on a GaAs wafer and was allowed to dry under ambient conditions in a fume hood.

Results

Carboxylate-terminated polystyrene spheres were modified with aminoethanethiol (AET), as shown schematically in Figure 1, to give thiol-terminated polystyrene spheres. Gold nanoparticles readily attached to these thiol-terminated polystyrene spheres, confirming the presence of thiol groups on the surface. The gold nanoparticles did not bind to carboxylate-terminated spheres that had not been modified with AET. Figure 2 shows TEM images of the polystyrene spheres after binding with \sim 12 nm diameter gold particles prepared using sodium citrate as the reducing agent (citrate-gold, Figure 2a) and 1–2 nm diameter particles produced using THPC as the reducing agent (THPC-gold, Figure 2b). These images show modest coverage of the polystyrene surface. Depending on the gold nanoparticle size and the gold-to-PS ratio, coverages of up to about 50% were achieved. Here, it may be noted that Westcott et al.³⁴ used aminobenzeneethiol as a linker to bind citrate-gold particles to a silica surface and achieved moderate coverage. They also noted that, in their case, aminoethanethiol worked with very poor efficiency as a linker.

The surfactant-coated gold nanoparticles are charged in aqueous solution. While this is important in allowing them to be dispersed, the resulting electrostatic repulsion prevents formation of a continuous shell directly by deposition of gold nanoparticles on the PS surface.

Further coverage was achieved by the reduction of gold hydroxide to grow the gold nanoparticles, which serve as seeds. Reduction of gold hydroxide by hydroxylamine hydrochloride took place on the surface of these (Au/AET/PS) particles. This resulted in a purple-blue solution, leaving some black precipitates at the bottom of the reaction vial. Occasionally it was found that the addition of hydroxylamine hydrochloride yielded simply a green solution but no precipitate. TEM imaging showed that the purple-blue solution consisted of relatively large gold particles (about 120 nm), while the black precipitate consisted of polystyrene particles covered with larger gold particles or gold shells. It was noted that formation of larger agglomerates of gold nanoparticles occurred if the initial ratio of gold hydroxide solution to Au/AET/PS particle solution was above about 25.

The nanoshells that formed using citrate-gold dressed Au/AET/PS have a rough surface because of the relatively large size of the citrate-gold nanoparticles (12 nm), as shown by their TEM images in Figure 3. These nanoshells

(31) Xu, H.; Tseng, C. H.; Vickers, T. J.; Mann, C. K.; Schlenoff, J. B. *Surf. Sci.* **1994**, *311*, 707.

(32) Weiser, H. B. *The Colloidal Elements*; Wiley: New York, 1933.

(33) Duff, D. G.; Baiker, A.; Gameson, I.; Edwards, P. P. *Langmuir* **1993**, *9*, 2310.

(34) Westcott, S. L.; Oldenburg, S. J.; Lee, T. R.; Halas, N. J. *Chem. Phys. Lett.* **1999**, *300*, 651.

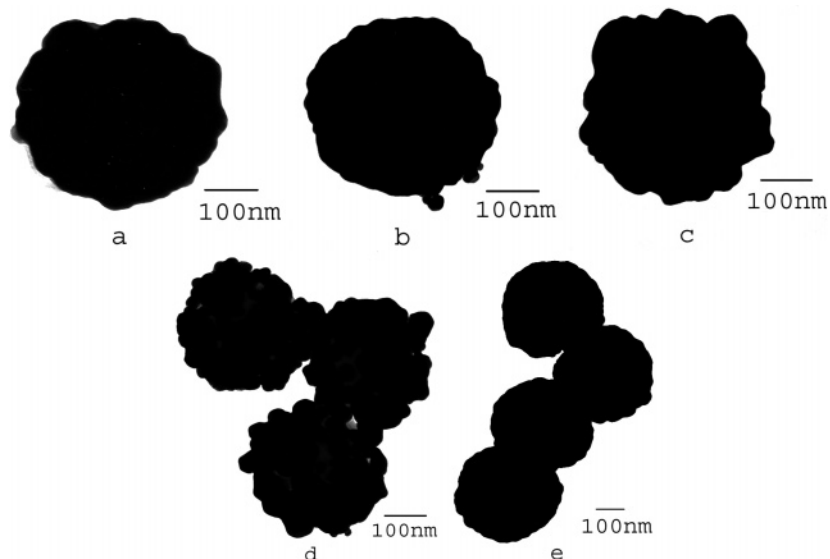


Figure 3. Rough gold shell/polystyrene core structures formed using citrate gold as the seeds for shell growth.

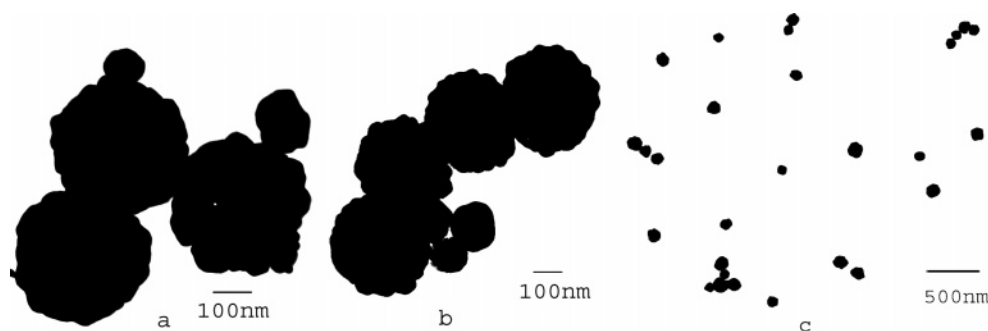


Figure 4. Rough nanoshells formed using citrate-gold, showing the simultaneous formation of large (~120 nm) free gold particles.

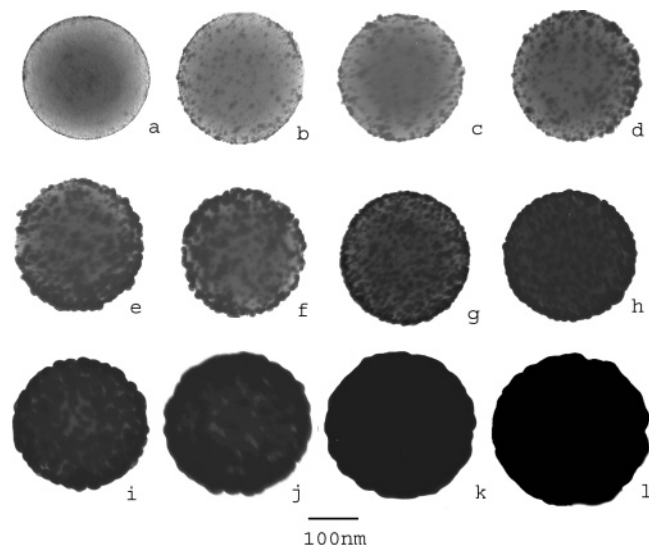


Figure 5. Sequence of TEM images showing the progressive growth of a complete gold shell on THPC-gold dressed PS spheres upon reduction of progressively greater quantities of gold hydroxide with hydroxylamine HCl.

tend to aggregate in solution and precipitate. In the process of growing a complete shell on these particles, many large gold particles (~120 nm) were simultaneously formed, as shown in the TEM images of Figure 4.

In contrast, the nanoshells formed using THPC-gold dressed Au/AET/PS have a relatively smooth surface (Figure 5k,l) and remained well-dispersed in water for many hours. After a prolonged time (more than 24 h), a

green precipitate that was readily redispersed by gentle shaking was formed. One notable point is that the neat monodispersed polystyrene readily crystallizes (self-assembles) into an ordered assembly (two- or three-dimensional). As the adsorbed gold particles render the surface somewhat rough, the long-range order breaks down and mostly isolated particles or their dimers or trimers are observed, rather than larger ordered clusters. Figure 6 shows accidental finding of trimers of gold-dressed polystyrene particles with gradually increasing surface coverage of gold that forms the basis for longer range ordered assemblies. Figure 7 shows a larger number of partially covered spheres to indicate the degree of sphere-to-sphere uniformity of coverage at this intermediate state of shell growth. The 25 or so spheres in this image all show about the same degree of gold coverage. Coverage remained similarly uniform at different spots on the TEM grid, and for samples with lesser or greater degree of coverage. Figure 8 shows an SEM image of a larger number of spheres, showing a limited degree of ordering. It is clear from this image that the surface roughness of the shells has inhibited the ability of the spheres to self-assemble into an ordered lattice. Future work will be required to optimize the process to prepare the metal shell without eliminating the capability of forming an ordered lattice structure. This may be realized by using even smaller gold particles and keeping a hydrophilic terminal group on the surface of gold to ensure aqueous dispersibility.

The extinction spectra of citrate-gold and THPC-gold dressed PS spheres with increasing ratios of gold:PS are presented in Figures 9a and 10a, respectively. As seen in

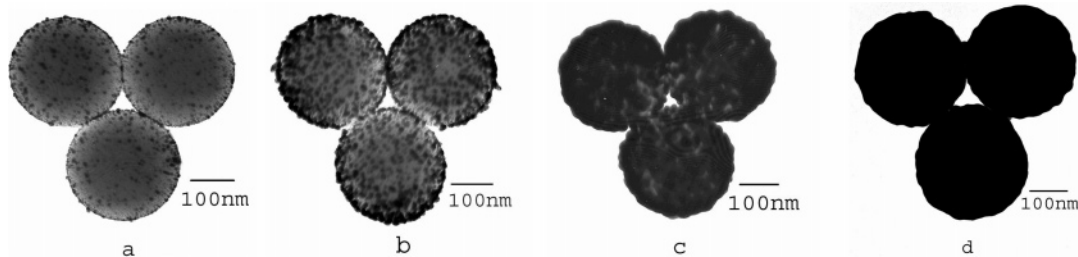


Figure 6. TEM images of polystyrene spheres with progressively greater gold coverage on their surface, showing their self-assembly into trimers with an equilateral triangle geometry that form the basis for larger ordered structures.

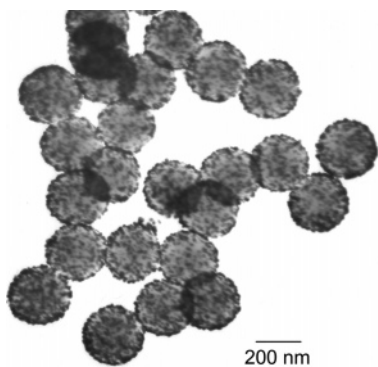


Figure 7. TEM image showing the uniformity of coverage of growing gold nanoparticles on polystyrene spheres.

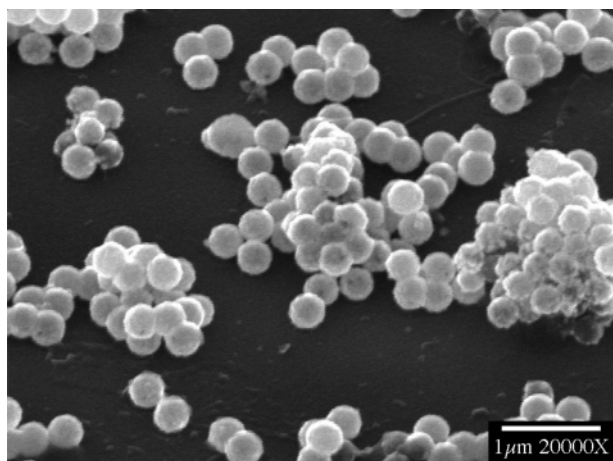


Figure 8. SEM image showing a large number of gold nanoshells.

Figure 9a, the SPR of citrate gold occurs prominently at 520 nm. As the gold coverage on citrate-gold seeded PS increases, the SPR absorption peak red shifts up to a maximum of 606 nm. This is accompanied by a substantial broadening of the SPR peak. In the case of THPC-gold, however, the SPR peak for neat gold particles is very broad, as seen in many earlier studies.³ With increasing coverage of the PS surface, seeded with THPC-gold particles, the SPR peak becomes more prominent and also red shifts up to 852 nm, as shown in Figure 10a. Once the surface is completely covered, forming a continuous shell, the peak no longer red-shifts. Further gold deposition, which results in increasing thickness of the shell, causes a blue-shift of the SPR extinction peak (Figure 10b). This is consistent with the findings of Oldenberg et al.⁹ Due to the broad nature of the peaks, the position of the extinction maximum in each case is more easily determined by examining the differentiated data, as shown in Figures 9b and 10c,d.

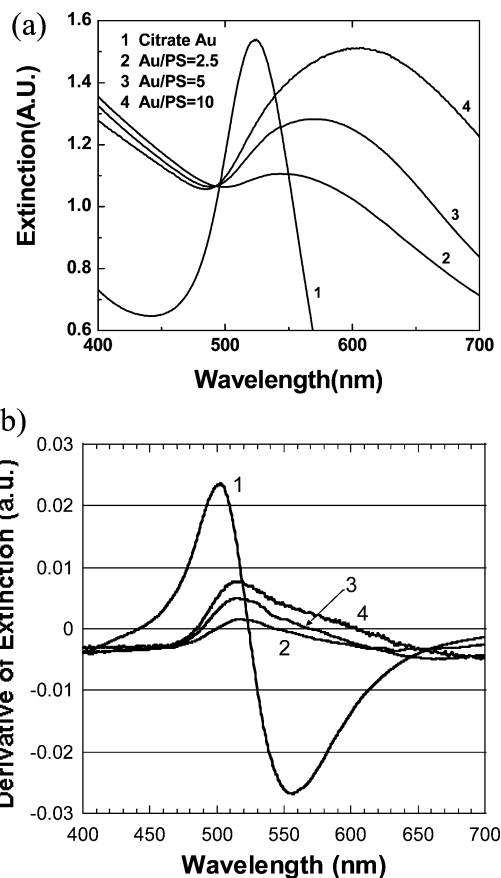


Figure 9. (a) Absorption spectra of citrate-gold dressed polystyrene particles (296 nm) with different coverage of gold particles resulting from different gold to PS ratios. (b) The same data, differentiated and smoothed for easier identification of the absorbance maxima. Curves 1–4 cross zero at 524, 543, 569, and 605 nm, respectively.

Discussion

In the present work, we have accomplished the surface modification of commercially available carboxylate-terminated polystyrene particles, using aminoethanethiol as a linker molecule. This allows the self-assembly of aqueous gold nanoparticles onto the surface of the former particles where they act as nucleation centers, eventually facilitating a complete coverage of the polystyrene sphere by a thin gold shell. Controlling the SPR of gold over a broad region of the electromagnetic spectrum by making a dielectric core-metal shell configuration was pioneered by Halas group.^{9,35} They have shown that much greater control of the SPR position can be achieved by adopting the present configuration compared to the reverse one, namely, metal core-dielectric shell where a shift of only

(35) Averitt, R. D.; Westcott, S. L.; Halas, N. J. *Phys. Rev. B* **1998**, *58*, 10203.

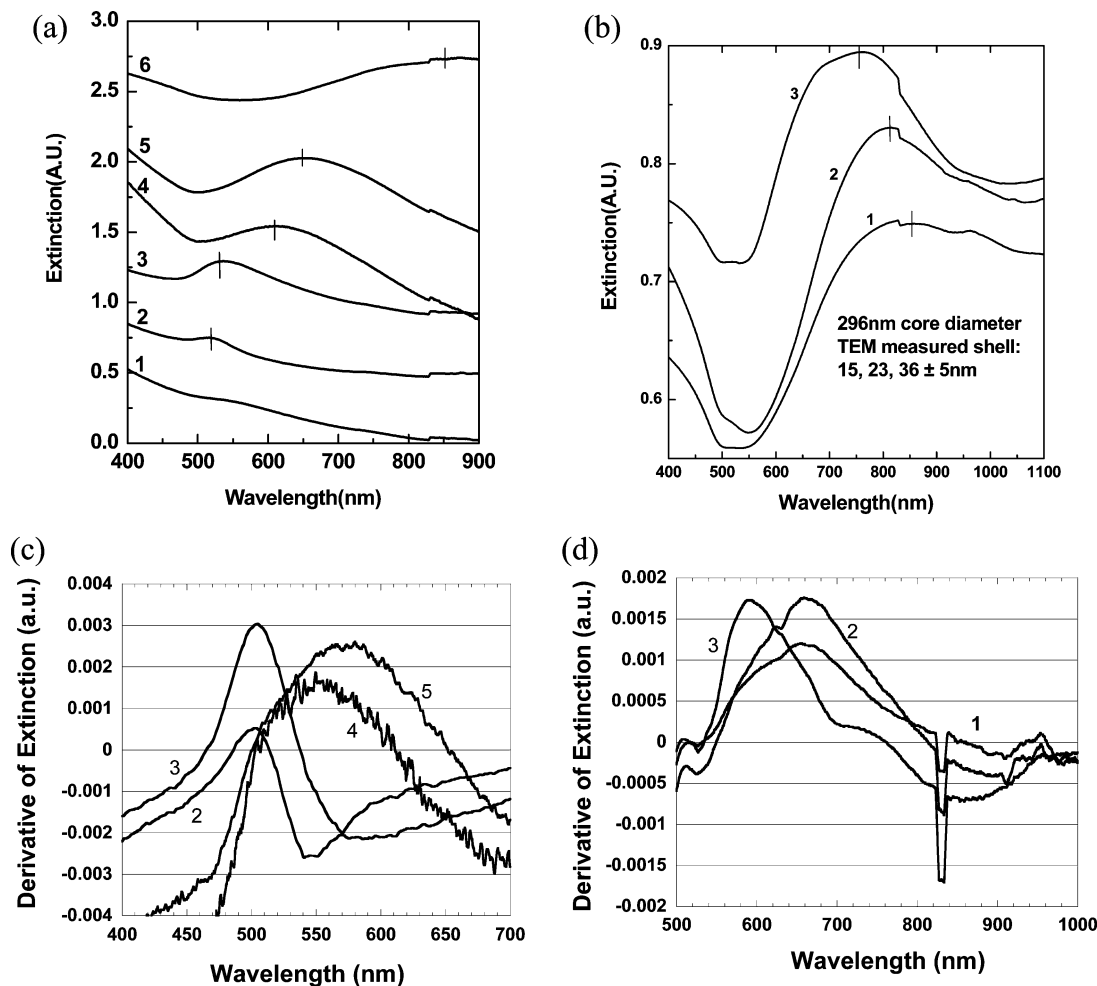


Figure 10. (a) Extinction spectra of THPC-gold dressed polystyrene particles (296 nm) after different amounts of shell growth. Curve 1 corresponds to images a and b in Figure 5; curve 5 corresponds to images g-i; and curve 6 corresponds to images j and k. Curves 1-5 follow the evolution of the optical absorption as coalescence of the gold layer progresses. (b) Extinction spectra of successively thicker THPC-gold derived shells. c and d show data from a and b, respectively, differentiated and smoothed for easier identification of the extinction maxima. In c, curves 2-5 cross zero at 514, 538, 571, and 652 nm, respectively. In d, curves 1-3 cross zero at 857, 814, and 762 nm, respectively. The step in the data near 820 nm is the result of a detector change in the spectrometer.

about 20 nm could be accomplished. In their work, they bound 1-2 nm diameter gold nanoparticles onto silica particles surface functionalized with 3-(aminopropyl)-triethoxysilane. The initial partial coverage increased into a full solid shell by reduction of gold precursor in the presence of these particles, where the attached gold acted as nucleating centers.⁹ In the preparation reported here, we have used aminoethanethiol as a linker molecule on the surface of carboxylate-terminated polystyrene to adapt this seed and grow method of nanoshell formation to use polystyrene, rather than silica, cores. In the first round of direct adsorption of gold nanoparticles, we also see only a partial surface coverage that could be systematically improved by seeded reduction of additional gold salt. With increasing gold coverage, the plasmon resonance red-shifts from that of isolated gold particles, near 520 nm, until the shell is complete. After the shell is complete, the plasmon resonance blue-shifts with increasing shell thickness. This, as observed by Goldenbergh et al. in the case of gold shells on silica cores, is understood in the framework of Mie scattering theory as increasing multipole contributions to the extinction become significant with increasing shell thickness.³²

For complete continuous shells, the extinction spectra can be compared to those predicted by the extended Mie scattering theory for core-shell particles as developed by

Aden and Kirker.³⁶ We have done so, using the formulation of the solution presented by Toon and Ackerman.³⁷ Parts a-c of Figure 11 compare the spectra shown in Figure 10b to these theoretical predictions. In computing the spectra, we have incorporated electron-interface scattering by using a size-dependent dielectric function for the gold shell, following the approach of Westcott et al.³⁸ We have used a value of 3 for the parameter A in their model, which accounts for the angular nature of electron scattering, scattering at grain boundaries in the polycrystalline shell, and the shape of the core-shell and shell-surroundings interfaces. The computed spectra do not account for the presence of a distribution of shell thicknesses that is inevitably present, nor for any effects resulting from shell roughness or deviation from a spherical shape. The predicted position and approximate width of the plasmon resonance peak in each of the extinction spectra is in good agreement with the experimental results. The experimental spectra do not show all of the structure predicted by the calculations, presumably due to variability in shell thickness and imperfections in the spherical core-shell geometry. Incorporation of a distribution of shell thick-

(36) Aden, A. L.; Kerker, M. *J. Appl. Phys.* **1951**, *22*, 1242.

(37) Toon, O. B.; Ackerman, T. P. *Appl. Opt.* **1981**, *20*, 3657.

(38) Westcott, S. L.; Jackson, J. B.; Radloff, C.; Halas, N. *J. Phys. Rev. B* **2002**, *66*, 155431.

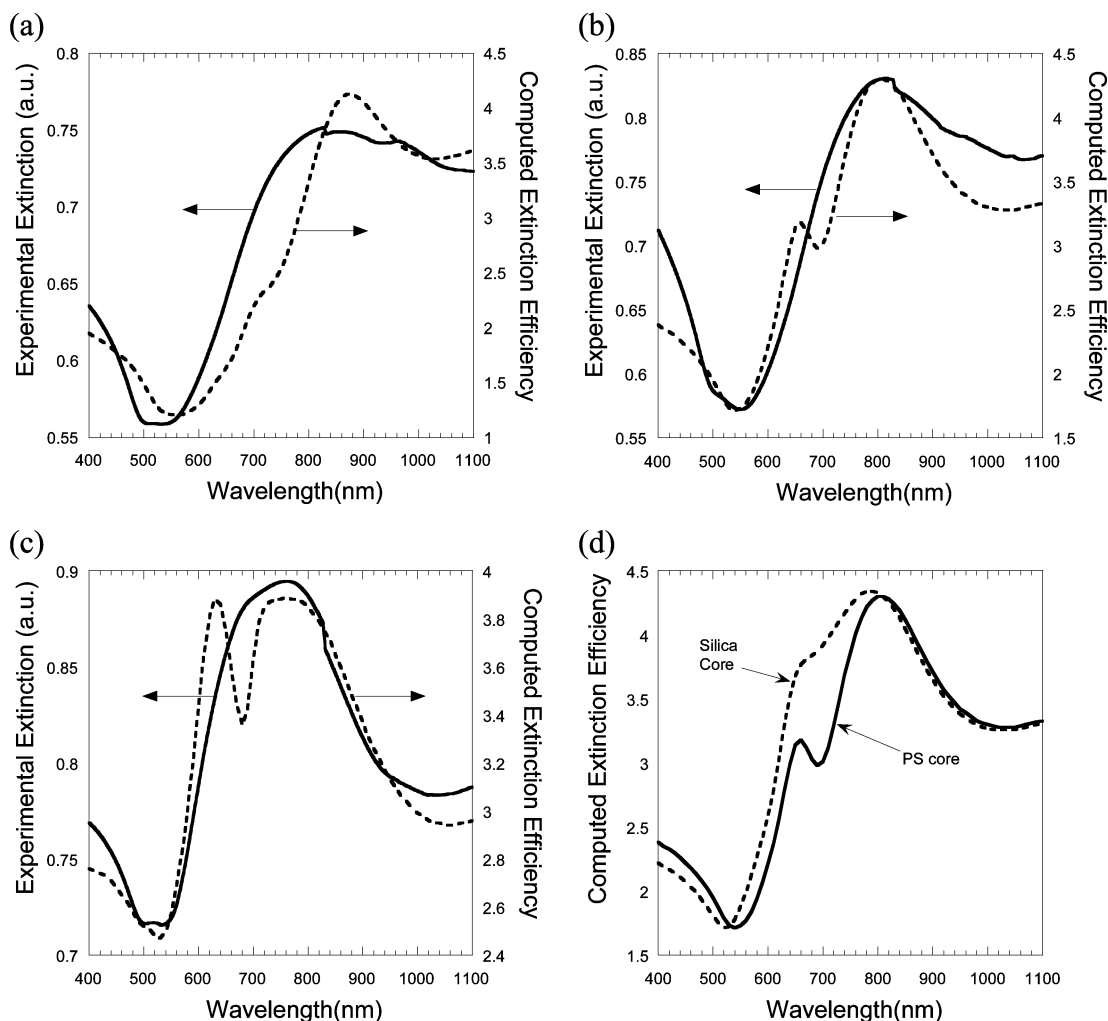


Figure 11. Comparison of experimental extinction spectra (solid lines in a–c) with extended Mie theory calculations (dashed lines in a–c): (a) 296 nm core diameter, 15 nm shell thickness; (b) 296 nm core diameter, 23 nm shell thickness; and (c) 296 nm core diameter, 36 nm shell thickness. Part d shows the computed spectra for a 23 nm shell on a core of silica (dashed line, index of refraction = 1.43) or polystyrene (solid line, index of refraction = 1.59).

nesses, with a standard deviation of 5 nm, into the calculated extinction spectra did not result in any dramatic change in the predicted spectra. Thus, the bulk of the difference between the experimental and calculated spectra must be attributed to other imperfections in the core–shell structures. Panel d of Figure 11 shows computed spectra for the 296 nm diameter core polystyrene (index of refraction = 1.59) and the same size silica (index of refraction of 1.43) with 23 nm gold shells. This demonstrates that, all other things being equal, the higher refractive index of the polystyrene core, compared to silica, results in a somewhat narrower peak in the extinction spectrum than that with a silica core.

These core–shell structures can be used as functional building blocks for incorporation into microstructures that are useful for coupling with electromagnetic radiation (antenna effect)³⁹ or can serve as candidates for producing organized structures such as photonic crystals. Core–shell colloidal materials, of which the present work is an example, have potential applications in electronics, photonics, catalysis, and diagnostics, etc. In particular, the possibility of tailoring the SPR absorption to the wavelength regions of 800–1300 nm, which have been demonstrated as the spectral region best suited for optical

bioimaging and biosensing applications, would make these materials suitable for direct bioapplications. As for photonic applications, where an organized three-dimensional structure is useful, the roughness of the surfaces of the core–shell particles would inhibit the required self-assembly to obtain such structures. However, an ability to surface-coat dielectric spheres of different refractive indices is a good first step toward such realization, of which the present work is an example. The use of polystyrene latex spheres as the dielectric cores in these applications may be advantageous because of their ready commercial availability at a wide range of sizes, with very high monodispersity, and with dyes or other organic molecules incorporated into them.

Conclusion

A method of synthesizing core–shell structures, consisting of monodispersed polystyrene latex cores with gold shells has been presented. Gold nanoparticles, ranging in size from 1 to 20 nm, were prepared by reduction of a gold precursor with reducing agents such as sodium citrate or tetrakis(hydroxymethyl)phosphonium chloride (THPC). Carboxylate-terminated polystyrene spheres were functionalized with 2-aminoethanethiol hydrochloride (AET), resulting in thiol-termination of their surface. Gold nanoparticles were then bound to the thiol groups to provide up to about 50% coverage of the surface. These

(39) Oldenburg, S. J.; Hale, G. D.; Jackson, J. B.; Halas, N. J. *Appl. Phys. Lett.* **1999**, *75*, 1063.

nanoparticles served as seeds for growth of a continuous gold shell. The shell thickness and roughness were controlled by the size of the nanoparticle seeds and by the procedure of their growth into a continuous shell. By variation of the thickness of the gold overlayer, relative to the size of the polystyrene core, the plasmon resonance of the nanoshell can be tuned to a specific wavelength across the visible and infrared range of the electromagnetic spectrum, which is useful for applications ranging from the construction of photonic crystals to biophotonics. The position and the width of the measured extinction spectra of these core-shell structures agreed well with the

predictions made using extended Mie scattering theory for such structures.

Acknowledgment. We are grateful to Joseph Haus of the University of Dayton for helpful discussions. This work was partially supported by a DURINT grant from the Chemistry and Life Sciences Division of the Air Force Office of Scientific Research and by the UB office of the Vice President for Research.

LA047628Y